Nanoscale

RSC Publishing

COMMUNICATION

View Article Online
View Journal | View Issue

Manipulating light absorption of graphene using plasmonic nanoparticles

Cite this: *Nanoscale*, 2013, **5**, 7785

Jinfeng Zhu,*[a] Qing Huo Liu*[ab] and Timothy Lin[c]

Received 22nd May 2013
Accepted 29th June 2013

DOI: 10.1039/c3nr02660d

www.rsc.org/nanoscale

We present the incorporation of periodic gold nanoparticle arrays into graphene-based photodetectors to enhance and tune light absorption of graphene. By the use of electromagnetic simulations, we show that light absorption in graphene can be manipulated by tuning plasmonic resonance. A maximum absorption of 30.3% with a full width of 135 nm at half maximum is achieved through systematic optimization of nanostructures.

Graphene, a single sheet of carbon atoms in a hexagonal lattice, has attracted a surge of interest due to its exceptional properties, including fast carrier mobility, high optical transparency, unique mechanical flexibility and strength.[1–4] Graphene is regarded as a promising alternative material compared with silicon for future optoelectronic devices.[5,6] Over the past few years, several graphene-based photodetectors have been demonstrated.[7–9] However, there are two intrinsic characteristics of graphene limiting its application in photodetection devices. First, the optical absorption of floated graphene is only about 2.3%,[10] which is intrinsically poor and results in low photoresponsivity. Second, graphene does not show spectral selectivity because of its wavelength-independent absorption from 300 nm to 2500 nm.[5] In order to overcome these two limitations, plasmonic nanostructures which are based on noble metals can be combined with graphene to boost the device performance through enhanced optical response.[11] Noble metal nanoparticles (NPs) can act as plasmonic nanoantennas to improve the performance of graphene-based photodetectors by near field excitation and hot electron contribution, as reported by Fang *et al.*[12,13] The use of gold NP arrays has demonstrated strong enhancement of photovoltage and photocurrent through enhanced visible light absorption in graphene-based photodetectors.[14,15] It has also been found that the visible spectra of enhanced absorption are tuneable by using localized surface plasmon resonance (LSPR) of gold NPs. Despite initial experimental studies, systematic modeling of the related nanostructures for graphene-based photodetectors is needed, in order to facilitate manipulation of the absorption enhancement and spectral selectivity by using particle plasmons.

In this paper, we theoretically investigate plasmonic effects of periodic gold NP arrays on graphene-based nanostructures and manipulate optical absorption in graphene by adjusting gold nanoantennas. Our study shows that plasmonic nanostructures can be well controlled to produce selective optical absorption enhancement, which is independent of the polarization of incident light. These results originate from the light concentration by LSPR and the electromagnetic coupling of gold nanoantennas.

In our modeling work, the periodic gold NP arrays are adhered to graphene on a SiO_2/Si substrate, as shown in Fig. 1. The thickness of silica and the pitch of NP arrays are denoted as t and p, respectively. The NP is assumed to be cuboid in shape with a bottom edge length of a and height h. The silica has a refractive index $n_0 = 1.46$. The frequency-dependent optical constants of gold NPs and silicon are extracted from experimental data reported in the literature.[16–18] All refractive media are assumed to be isotropic. Electromagnetic simulations are performed to investigate the optical absorption in graphene using the 3-dimensional finite-difference time-domain method, which solves Maxwell's equations in complex geometries numerically.[19] In consideration of the periodic boundary conditions (PBCs) and electromagnetic symmetries, we only need to discuss the normally incident plane wave with x-polarization. The perfectly matched layers (PMLs) are used as artificial absorbing layers to simulate optical open boundary conditions. The non-uniform mesh is applied in all simulations.

In order to simulate its optical response in the visible range, graphene is assumed to be an effective electromagnetic

[a]*Department of Electronic Science, Xiamen University, Xiamen 361005, China. E-mail: nanoantenna@hotmail.com; Qing.Liu@duke.edu*

[b]*Department of Electrical and Computer Engineering, Duke University, Durham, NC 27708, USA*

[c]*Aegis Technology Inc., 12630 G Westminster Ave., Santa Ana, CA 92706, USA*

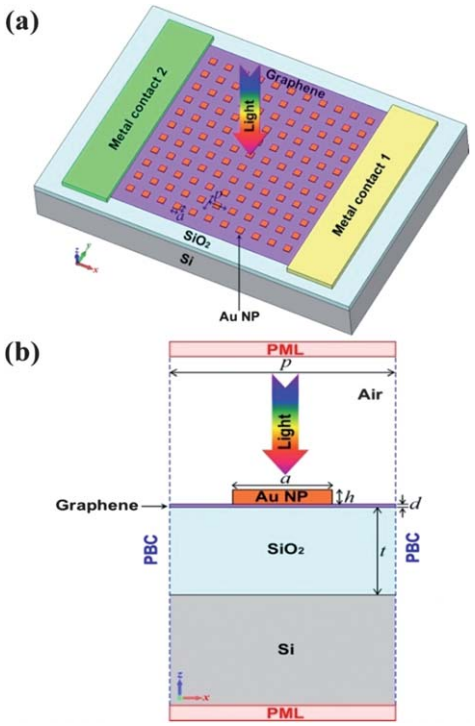

Fig. 1 (a) Schematic drawing of a graphene-based photodetector with plasmonic NPs. (b) Side view of the simulated nanostructure.

medium with a homogeneous film of thickness $d = 0.34$ nm. Based on the framework of Fresnel coefficients approach,[20] the refractive index $\tilde{n}(\omega)$ of graphene can be defined by eqn (1) and (2):

$$\tilde{n}(\omega) = n(\omega) + ik(\omega) \quad (1)$$

$$k = -\frac{c}{2\omega dn}\ln[1 - \pi\alpha], \quad n = 3.0 \quad (2)$$

where $\tilde{n}(\omega)$ is a complex-valued function of angular frequency ω, n is the real part of the refractive index, k is the extinction coefficient and determines the optical absorption in graphene. In the visible range, the absorption spectrum of graphene is quite flat, so n is assumed to be constant. In eqn (2), c is the speed of light in vacuum, and the fine structure constant is defined as $\alpha \approx 1/137$.[10] The optical absorption of graphene at angular frequency ω is calculated by eqn (3),

$$A(\omega) = 2\omega nk\int_V |E|^2 \mathrm{d}V' \quad (3)$$

where E is the local electric field, V is the volume of graphene, $\omega = 2\pi c/\lambda$, and λ is the free space wavelength. The effects of saturable absorption and heat disturbance in graphene are not considered in the modeling. In order to validate the modeling approach, we simulate the optical transmission of floated graphene and compare it with experimental results from ref. 10, as shown in Fig. 2. The comparison demonstrates that the transmission through graphene is about 97.7%, consistent with the experimental data. The simulation results also indicate that the reflectance is negligible and graphene only absorbs about 2.3%

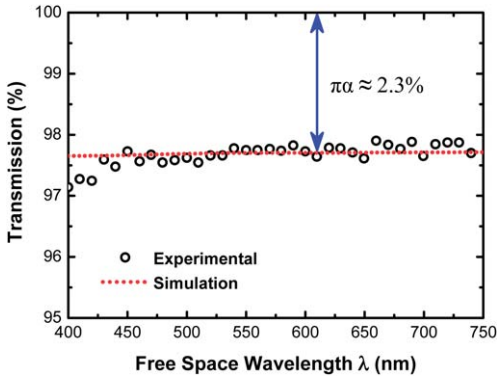

Fig. 2 Visible light transmission of floated graphene.

of incident light, which is in agreement with the fine structure constant α, as shown in Fig. 2.

The purpose of our study is to excite plasmonic resonance to confine selective light energy inside graphene. The plasmonic resonance of gold NP arrays is influenced by particle shapes and sizes, environmental dielectric media, substrate effects, and interparticle electromagnetic coupling.[21–23] Taking advantage of these effects, one can manipulate the light absorption of graphene by tuning the plasmonic resonance within the visible spectrum.

First of all, we consider the general effect of the silica dielectric layer on light absorption of graphene. It has been found that the thickness of silica between graphene and the reflective substrate Si can be adjusted to tune the optical reflection from graphene.[24] Here, we compare the optical absorption of graphene using different thicknesses of silica in simulation models, as shown in Fig. 3(a). The graphene on a SiO_2/Si substrate without Au NPs exhibits interferometric absorption due to the phase delay of the reflective wave from graphene compared to the reflective wave from Si. The phase delay can be expressed as below,

$$\Delta\varphi = n_0\frac{2\pi}{\lambda}2t + \varphi_1 - \varphi_2 \quad (4)$$

where φ_1 and φ_2 are the reflective phase shift of π on the SiO_2/Si interface and the air–graphene interface, respectively, and $\varphi_1 - \varphi_2 = 0$. Due to the interference effects, the maximum reflection and minimum absorption from graphene occur at $\Delta\varphi = 2m\pi$, and the maximum absorption emerges at $\Delta\varphi = (2m - 1)\pi$, where m is a positive integer. For instance, when t is set to 300 nm in the simulation, graphene obtains the minimum absorption at $\lambda = 438$ nm ($\Delta\varphi = 4\pi$), and the maximum absorption at $\lambda = 584$ nm ($\Delta\varphi = 3\pi$), as shown in Fig. 3(a). In order to achieve optimal enhanced absorption using Au NPs, the effects of optical interference and plasmonic resonance should both be considered for the design of nanostructures. When the intrinsic interferometric absorption peak is matched with the plasmonic resonance wavelength, the enhanced near field efficiently contributes to the optical loss inside graphene. Therefore, optimal absorption enhancement is implemented. As shown in Fig. 3(b), for $t = 300$ nm, the maximum absorption of Au NPs due to plasmonic resonance and the intrinsic

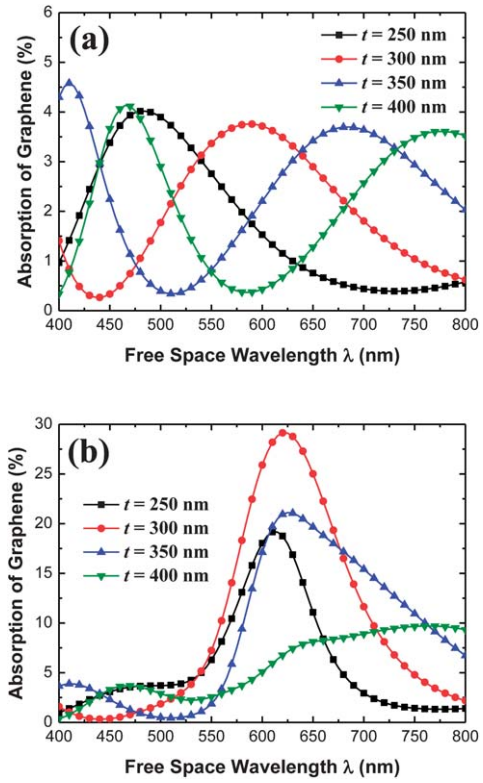

Fig. 3 Light absorption in graphene using different thicknesses of silica. (a) Without Au NPs and (b) with Au NPs for $p = 120$ nm, $a = 50$ nm and $h = 20$ nm.

absorption peak due to optical interference are perfectly matched at $\lambda = 584$ nm, hence a broader absorption band with the strongest absorption efficiency of 29.2% is obtained, and the FWHM has a value of 116 nm. For $t = 400$ nm, the absorption shows weaker enhancement without an obvious peak because of the serious mismatch between interference and plasmonic resonance. In order to simplify our theoretical analysis, we use silica of thickness 300 nm in the following discussion.

Next, the influence of gold particle height h on the absorption of graphene is investigated. As shown in Fig. 4, the absorption spectra of graphene demonstrate strong enhancement because of plasmonic resonance by using gold NP arrays.

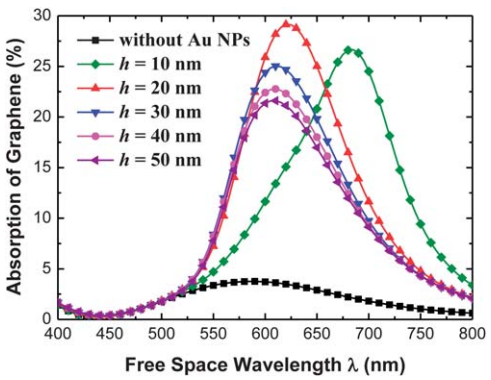

Fig. 4 Light absorption of graphene using different heights of Au NPs, for $t = 300$ nm, $p = 120$ nm and $a = 50$ nm.

The spectra are blue-shifted from 684 nm to 609 nm as h increases from 10 nm to 50 nm. The spectrum shift is attributed to the change of plasmonic resonance wavelength by manipulating the height of Au NPs. Fig. 4 also indicates that the absorption peak maxima is obtained at $\lambda = 620$ nm when h has a value of 20 nm. The mechanism of absorption enhancement can be interpreted using the electric field distribution analysis, as shown in Fig. 5. This figure for the electric field distributions indicates that absorption enhancement is attributed to the effect of plasmonic light concentration by using Au NPs.[25,26] Because graphene is ultrathin compared with Au NPs, the optical near field induced by plasmonic resonance is efficiently enhanced and concentrated in the graphene layer, as shown in Fig. 5(a)–(d). It is also observed from Fig. 5(a) and (b) that the electric field in between Au NPs and graphene is concentrated to the maximal degree around the plasmonic resonance wavelength of $\lambda = 584$ nm. At this wavelength, Au NPs have the absorption peak induced by LSPR (not shown here). However, the absorption maxima in graphene occurs at $\lambda = 620$ nm but not at the plasmonic resonance wavelength of Au NPs. This result can be explained by further comparing the electric field distributions surrounding graphene for the two wavelengths in Fig. 5(a)–(d). Fig. 5(a) and (b) show that the electric field is more concentrated in Au NPs at $\lambda = 584$ nm, which results in greater absorption in Au NPs and less enhanced absorption in graphene. In contrast, Fig. 5(c) and (d) demonstrate that a stronger near field is concentrated and well-distributed in graphene and creates much optical loss in it, at $\lambda = 620$ nm. At $\lambda = 440$ nm, there is no strong near field for absorption enhancement because it is far beyond the plasmonic resonance wavelength, as shown in Fig. 5(e) and (f).

We also consider the effects of the NP bottom edge length a and array pitch p on the optical absorption enhancement in graphene. The plasmonic resonance peak locations can be engineered to tune the optical absorption in graphene by manipulating NP sizes and array pitches.[27] It is observed in Fig. 6 that the absorption spectra of graphene have a red shift when a is increased or p is reduced. Besides, the absorption band becomes wider as the NP fill factor a^2/p^2 is higher. The red shift and band broadening are attributed to the coupling between localized plasmons. When the NP size is much smaller

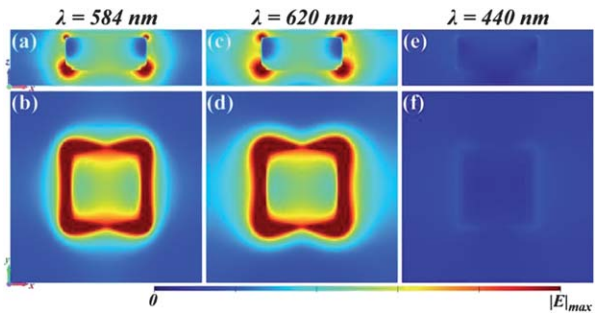

Fig. 5 Electric field distributions when $t = 300$ nm, $p = 120$ nm, $a = 50$ nm, and $h = 20$ nm. (a), (c) and (e) are the x–z cross-sections cutting through the cuboid Au NPs. (b), (d) and (f) are x–y cross-sections on the interface between the Au NPs and graphene.

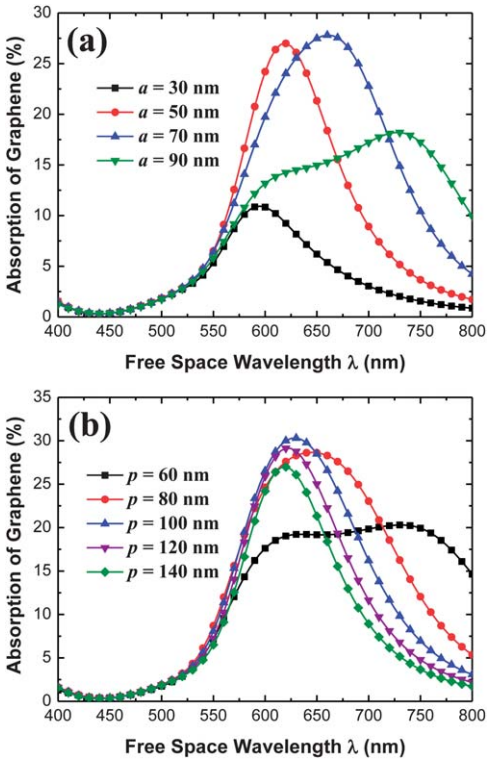

Fig. 6 Light absorption of graphene when $t = 300$ nm and $h = 20$ nm. (a) Using different bottom edge lengths of Au NPs for $p = 140$ nm. (b) Using different NP array pitches for $a = 50$ nm.

than the array pitch the electromagnetic interactions between Au nanoantennas can be neglected and the absorption in graphene shows weak enhancement, because the strong near field in graphene is highly concentrated surrounding the bottom edges of Au NPs. This is shown in Fig. 6(a), with $a = 30$ nm and $p = 140$ nm. As the fill factor becomes larger, electromagnetic coupling between NPs strengthens the intensity of optical near field in the part of graphene where no Au NPs are located. This enhances the absorption capability of graphene until it reaches the maximum spectrum peak at an optimum particle density. As shown in Fig. 6(b), when $a = 50$ nm and $p = 100$ nm the maximum absorption is 30.3% at $\lambda = 620$ nm (with FWHM = 135 nm). A high fill factor, such as $a = 50$ nm and $p = 60$ nm in Fig. 6(b), lowers the absorption peak and extremely extends the band width as a result of strong particle plasmon coupling between Au nanoantennas.

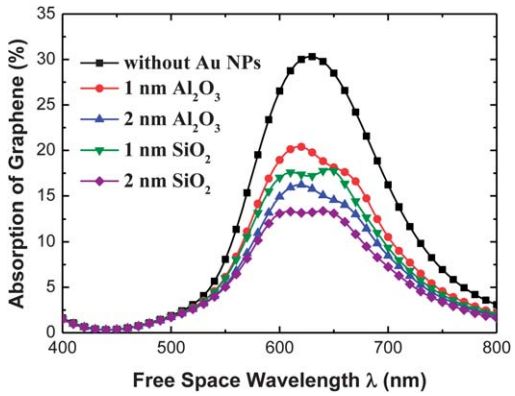

Fig. 7 Influence of insulator spacers on light absorption of graphene.

In real device applications, carrier transport and exciton recombination on the interface between Au NPs and graphene might significantly lower the quantum efficiency of photodetectors. So the transparent insulator spacers can be used to isolate Au NPs from graphene. We investigate the influence of using SiO_2 and Al_2O_3 spacers (the refractive index of Al_2O_3 $n_1 = 1.76$), as shown in Fig. 7. The absorption spectra of using insulator spacers have a small blue shift because they have a lower refractive index than graphene. Due to near-field effects of LSPR, absorption enhancement is weakened by increasing the thickness of the spacers. The maximum absorption of using 1 nm thick alumina is reduced by 33% compared to that without using spacers. Using Al_2O_3 spacers creates higher absorption enhancement than SiO_2 spacers when the same thickness of the insulator is used. This is because Al_2O_3 has a higher refractive index and concentrates more optical near-field energy inside graphene. The suitable isolating material with a high refractive index can be developed to ensure even higher absorption enhancement.

In summary, we investigate the incorporation of periodic gold nanoantennas into graphene-based photodetectors for boosting the device performance through light absorption enhancement and selectivity. The light absorption can be manipulated through plasmonic near-field engineering by controlling the thickness of silica, the size and array pitch of Au NPs, and the insulator spacers. The modeling work also implies that the light absorption spectrum of graphene can be adjusted by selecting other dielectric materials and metal nanoparticles in the design of nanostructures. Our investigation provides a guide for the device design of using plasmonic effects to improve the optical response of graphene. The research work also shows promising potential to develop low pass, band pass, and high pass graphene optoelectronic devices based on plasmonic hybrid nanostructures. The high absorption efficiency and spectral selectivity by designing plasmonic nanoantennas are achieved with graphene photodetector applications in mind, but the results are also relevant for the development of a wide variety of active nanophotonic components, such as graphene-based switches, modulators and sensors.

Acknowledgements

The authors acknowledge the support from the Institute of Electromagnetics and Acoustics at Xiamen University. Jinfeng Zhu thanks Dr Bo Zhao from Wave Computation Technologies, Inc. for helpful discussion.

Notes and references

1 K. I. Bolotin, K. J. Sikes, Z. Jiang, M. Klima, G. Fudenberg, J. Hone, P. Kim and H. L. Stormer, *Solid State Commun.*, 2008, **146**, 351.
2 C. Lee, X. Wei, J. W. Kysar and J. Hone, *Science*, 2008, **321**, 385.

3 K. S. Kim, Y. Zhao, H. Jang, S. Y. Lee, J. M. Kim, K. S. Kim, J.-H. Ahn, P. Kim, J.-Y. Choi and B. H. Hong, *Nature*, 2009, **457**, 706.
4 S. M. Kim, E. B. Song, S. Lee, J. Zhu, D. H. Seo, M. Mecklenburg, S. Seo and K. L. Wang, *ACS Nano*, 2012, **6**, 7879.
5 F. Bonaccorso, Z. Sun, T. Hasan and A. C. Ferrari, *Nat. Photonics*, 2010, **4**, 611.
6 Q. Bao and K. P. Loh, *ACS Nano*, 2012, **6**, 3677.
7 F. Xia, T. Mueller, Y. Lin, A. Valdes-Garcia and P. Avouris, *Nat. Nanotechnol.*, 2009, **4**, 839.
8 T. Mueller, F. Xia and P. Avouris, *Nat. Photonics*, 2010, **4**, 297.
9 M. C. Lemme, F. H. L. Koppens, A. L. Falk, M. S. Rudner, H. Park, L. S. Levitov and C. M. Marcus, *Nano Lett.*, 2011, **11**, 4134.
10 R. R. Nair, P. Blake, A. N. Grigorenko, K. S. Novoselov, T. J. Booth, T. Stauber, N. M. R. Peres and A. K. Geim, *Science*, 2008, **320**, 1308.
11 A. N. Grigorenko, M. Polini and K. S. Novoselov, *Nat. Photonics*, 2012, **6**, 749.
12 Z. Fang, Z. Liu, Y. Wang, P. M. Ajayan, P. Nordlander and N. J. Halas, *Nano Lett.*, 2012, **12**, 3808.
13 Z. Fang, Y. Wang, Z. Liu, A. Schlather, P. M. Ajayan, F. H. L. Koppens, P. Nordlander and N. J. Halas, *ACS Nano*, 2012, **6**, 10222.
14 T. J. Echtermeyer, L. Britnell, P. K. Jasnos, A. Lombardo, R. V. Gorbachev, A. N. Grigorenko, A. K. Geim, A. C. Ferrari and K. S. Novoselov, *Nat. Commun.*, 2011, **2**, 458.
15 Y. Liu, R. Cheng, L. Liao, H. Zhou, J. Bai, G. Liu, L. Liu, Y. Huang and X. Duan, *Nat. Commun.*, 2011, **2**, 579.
16 P. B. Johnson and R. W. Christy, *Phys. Rev. B*, 1972, **6**, 4370.
17 E. D. Palik, *Handbook of Optical Constants of Solids*, Academic, New York, 1985.
18 U. Kreibig and M. Vollmer, *Optical Properties of Metal Clusters*, Springer, Berlin, 1995.
19 A. Taflove and S. C. Hagness, *Computational Electrodynamics*, Artech House, Boston, 2000.
20 M. Bruna and S. Borini, *Appl. Phys. Lett.*, 2009, **94**, 031901.
21 B. P. Rand, P. Peumans and S. R. Forrest, *J. Appl. Phys.*, 2004, **96**, 7519.
22 J. Zhu, B. Zeng, R. S. Kim and Z. Wu, *Proc. SPIE*, 2011, **8333**, 83331C.
23 R. S. Kim, J. Zhu, J. H. Park, L. Li, Z. Yu, H. Shen, M. Xue, K. L Wang, G. Park, T. J. Anderson and Q. Pei, *Opt. Express*, 2012, **20**, 12649.
24 P. Blake, E. W. Hill, A. H. Castro Neto, K. S. Novoselov, D. Jiang, R. Yang, T. J. Booth and A. K. Geim, *Appl. Phys. Lett.*, 2007, **91**, 063124.
25 J. Zhu, M. Xue, H. Shen, Z. Wu, S. Kim, J. Ho, A. Hassani-Afshar, B. Zeng and K. L. Wang, *Appl. Phys. Lett.*, 2011, **98**, 151110.
26 J. Zhu, M. Xue, R. Hoekstra, F. Xiu, B. Zeng and K. L. Wang, *Nanoscale*, 2012, **4**, 1978.
27 M. L. Brongersma and P. G. Kik, *Surface Plasmon Nanophotonics*, Springer, Berlin, 2007.